Support materials

S1: Bayesian model comparison for unidirectional influence

These results for Table 3 can be interpreted in terms of the median (less prone to outliers than the mean) of the maximized free energy depicted in Figs. 11, 12 and 13. For instance, regarding the L-DCM and D-DCM algorithms, a relatively higher false model identification rate occurred when the ground truth is M2, as expected. This is mainly due to the fact that the difference between the median of the maximized free energy of M6, M10 or M16 models and the one of the M2 one is significantly small (see Fig. 11). Now, the DCM shows higher false model identification rate compared to the L-DCM and D-DCM methods. This can be interpreted by the highest median of the maximized free energy obtained for the M16 model. Regarding the correct model M5, as the medians of the maximized free energy of models M5, M6, M7 and M8 are to some extent comparable (see Fig. 12), with slight superiority for M5, some false model identification can occur for the three algorithms. As far as the ground truth M6 is concerned, Table 3 clearly shows very high performance in terms of detection rate, especially for D-DCM (99%) and DCM (97%). These results can also be interpreted in terms of the median of the maximized free energy depicted in Fig. 13. According to this figure, the median of the maximized free energy obtained for identifying the correct model, M6, for D-DCM and DCM algorithms, is significantly higher than the ones related to the other model structures. Consequently, a very low false detection rate for these algorithms is expected.

As relatively high false detection rate is to some extent problematic, investigating the model evidence, $p(\tilde{\boldsymbol{g}}|\mathrm{M}m)$, would help to complete the whole scene regarding the ability of each algorithm in identifying the model structure. This model evidence is nothing else than the model posterior probability under flat prior and Mm [40]. This quantity is computed via the softmax function of the median of the maximized free energy computed over the 100 conducted trials, that means: $p(\tilde{\boldsymbol{g}}|\mathrm{M}m) = \frac{\exp(\tilde{F}_m)}{\sum_{i=1}^{16}\exp(\tilde{F}_i)}$ where $\tilde{F}_i$ denotes the median of the maximized free energy associated to the model structure Mi. It is clear

from Figs. 11, 12 and 13 that the model evidence measure allows for a global quantification of the ability of the different algorithms in identifying the correct model structure except in ground truth M2 where M16 is identified using DCM.

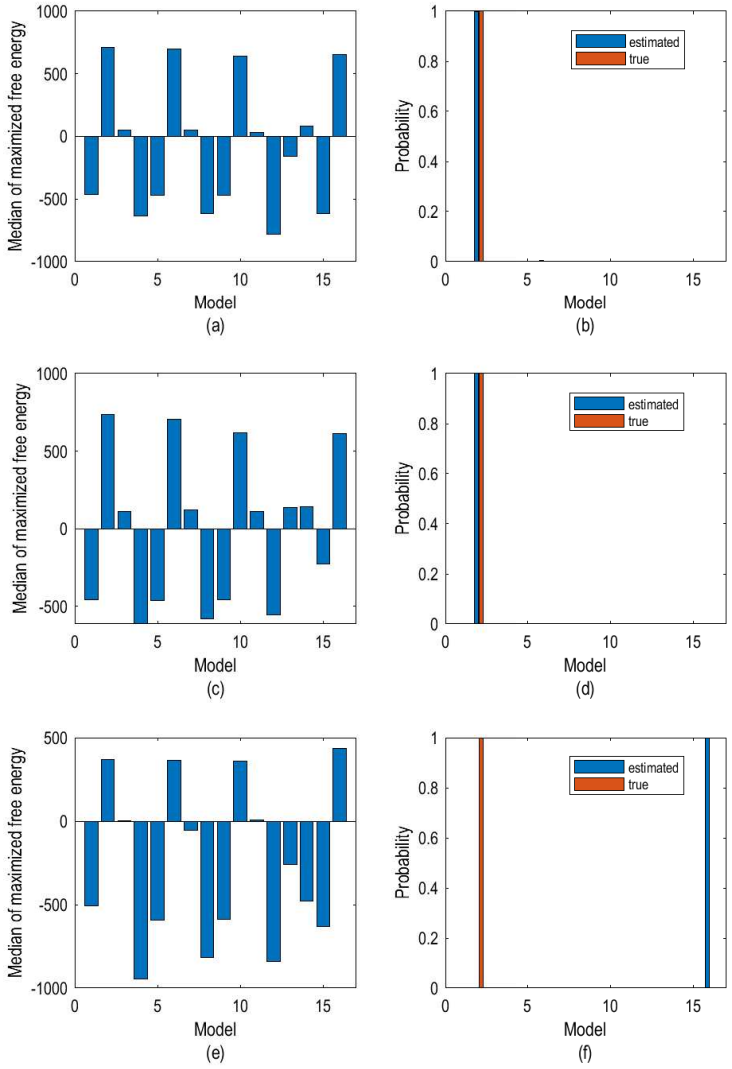

Figure 11. Bayesian model comparison in terms of the median of maximized free energy over 100 trials and the model posterior probability using **(a-b)** L-DCM, **(c-d)** D-DCM and **(e-f)** DCM for the ground truth M2 in the context of unidirectional influence.

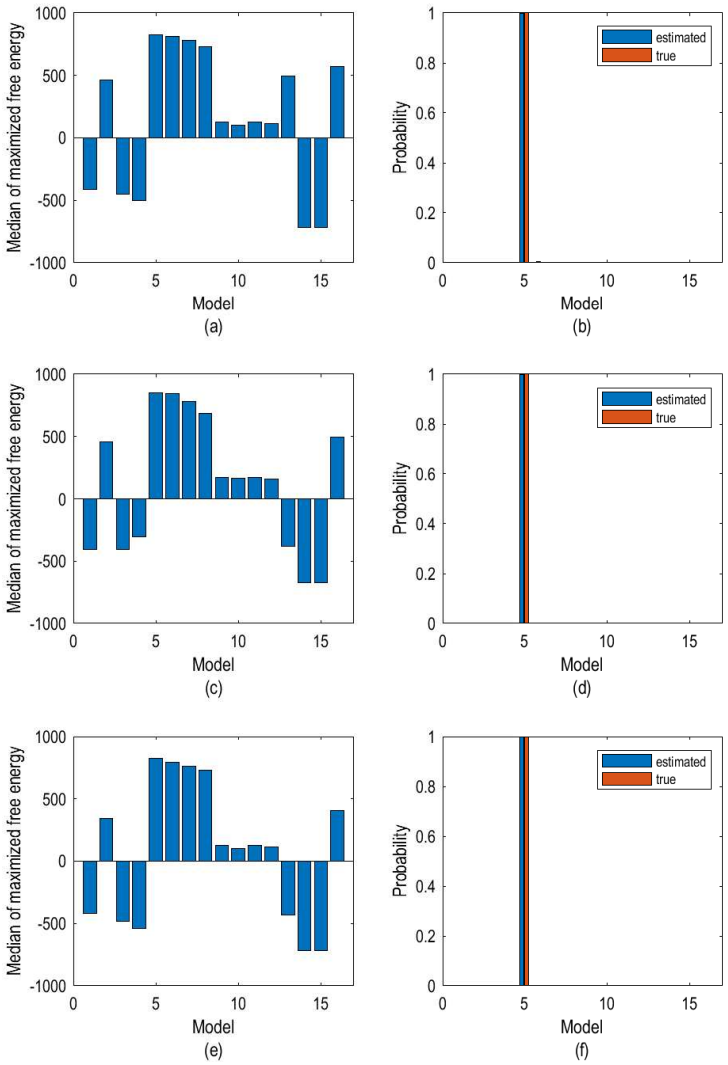

Figure 12. Bayesian model comparison in terms of the median of maximized free energy over 100 trials and the model posterior probability using **(a-b)** L-DCM, **(c-d)** D-DCM and **(e-f)** DCM for the ground truth M5 in the context of unidirectional influence.

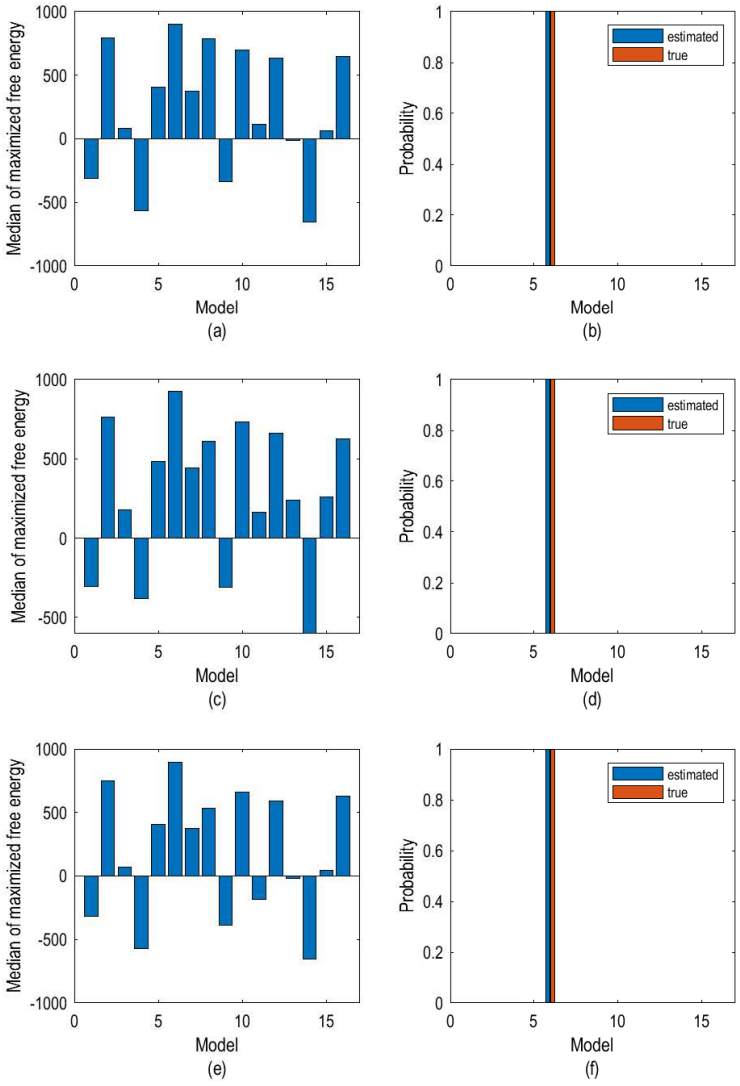

Figure 13. Bayesian model comparison in terms of the median of maximized free energy over 100 trials and the model posterior probability using **(a-b)** L-DCM, **(c-d)** D-DCM and **(e-f)** DCM for the ground truth M6 in the context of unidirectional influence.

S2: Bayesian model comparison for bidirectional influence

The results for Table 5 can be furthermore interpretable in Figs. 14, 15 and 16, which show the results of model selection based on the median of the maximized free energy over 100 Monte Carlo trials corresponding to ground truths M8, $M16_s$ and $M16_{as}$ respectively. Clearly, the correct model structure can be identified with almost 100% model posterior probability by all techniques as shown in these figures. As shown in Fig. 14, on the one hand, the gap on the median of the maximized free energy between the optimal model structure M8 and the model structure M16 (the model structure giving the second more important free energy among the 16 model structures) is small (< 30 for D-DCM and DCM) leading to the false detection of model structure (M16). On the other hand, this gap is slightly higher for L-DCM than for D-DCM and DCM, leading to a reduced false detection rate of M16 for L-DCM (14% *vs* 19% and 21% respectively), as shown in Table 5. A quite comparable behaviour of the three algorithms can be observed in the ground truth $M16_s$ (see Fig. 15), such that the gap on the median of the maximized free energy between the optimal model structure M16 and the model structure M8 (resp. M12) (the two model structures giving the second and third more important free energies among the 16 model structures) is small, this gap between M16 and M8 (resp. M12) is slightly higher for D-DCM than for DCM and L-DCM, leading to a reduced false detection rate of M8 (resp. M12) for D-DCM, DCM and L-DCM *i.e.* 2% *vs* 5% and 11% respectively (resp. 2% *vs* 1% and 9% respectively) as displayed in Table 5. Furthermore, as depicted in Fig. 16 where model structure $M16_{as}$ stands for the ground truth, the gap on the median of the maximized free energy between the optimal model structure M16 and the model structure M10 (the model structure giving the second more important free energy among the 16 model structures in this situation) is significant (higher than 270) whatever the method. The optimal model structure (M16) has a greater model posterior probability than any other model structure, so that 100% model identification rate is obtained by all techniques in this case (see Table 5).

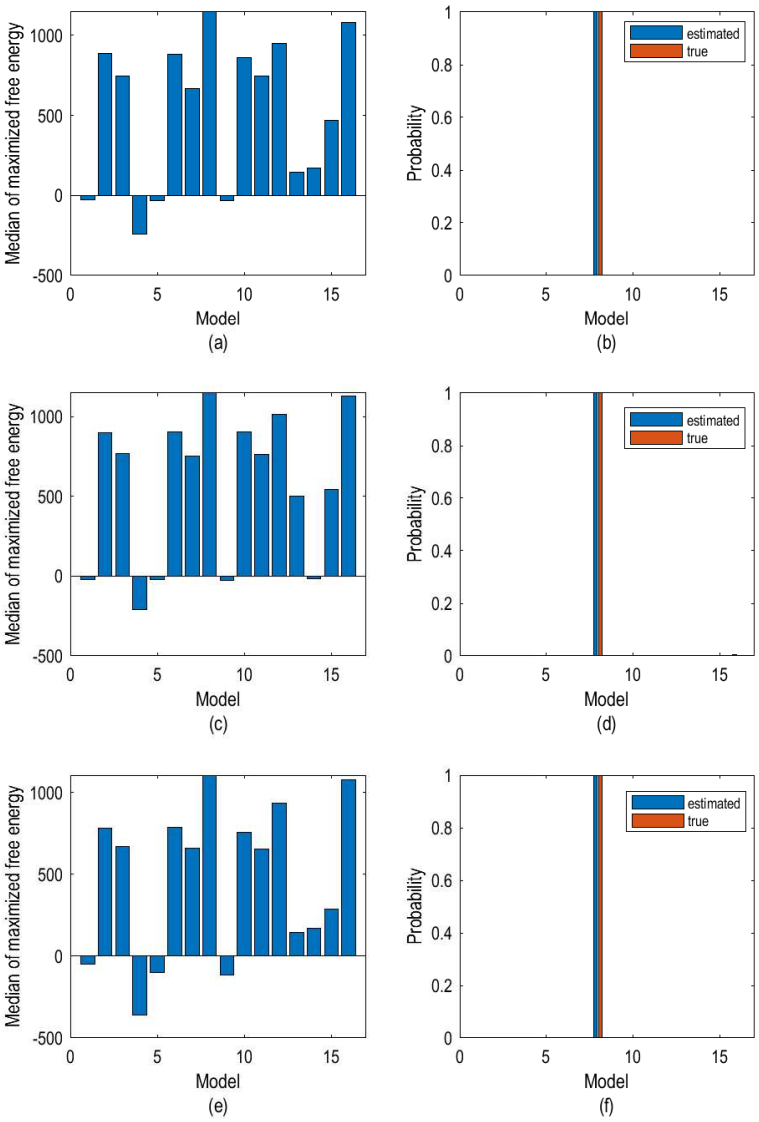

Figure 14. Bayesian model comparison in terms of the median of maximized free energy over 100 trials and the model posterior probability using **(a-b)** L-DCM, **(c-d)** D-DCM and **(e-f)** DCM for the ground truth M8 in the context of bidirectional influence.

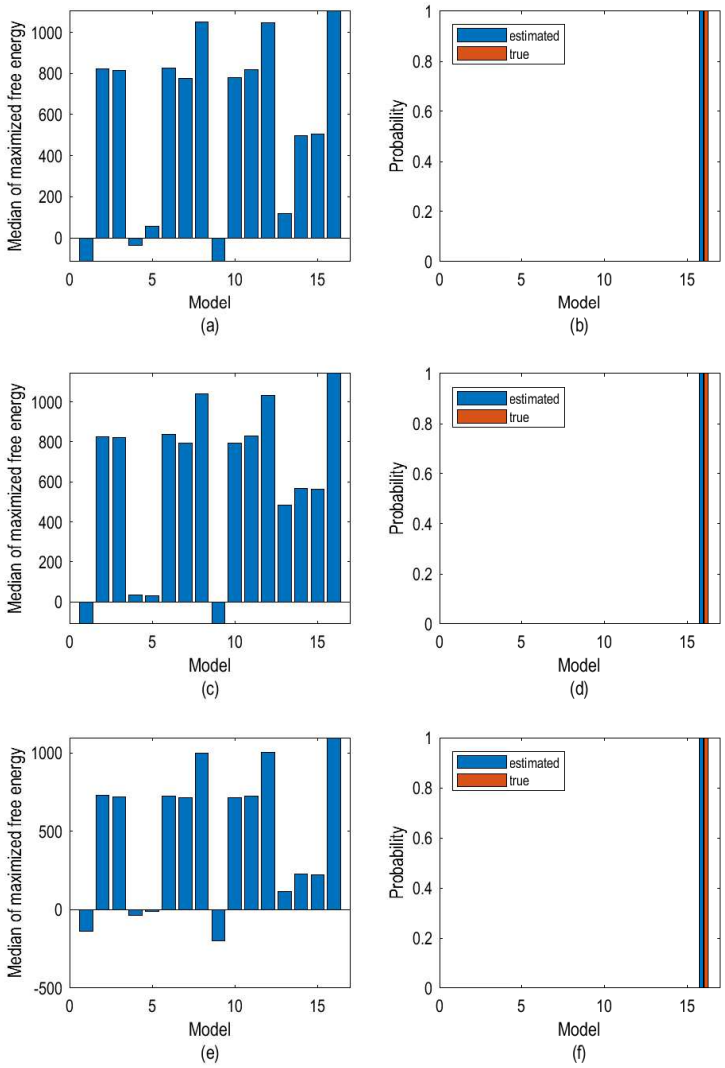

Figure 15. Bayesian model comparison in terms of the median of maximized free energy over 100 trials and the model posterior probability using **(a-b)** L-DCM, **(c-d)** D-DCM and **(e-f)** DCM for the ground truth $M16_s$ in the context of bidirectional influence.

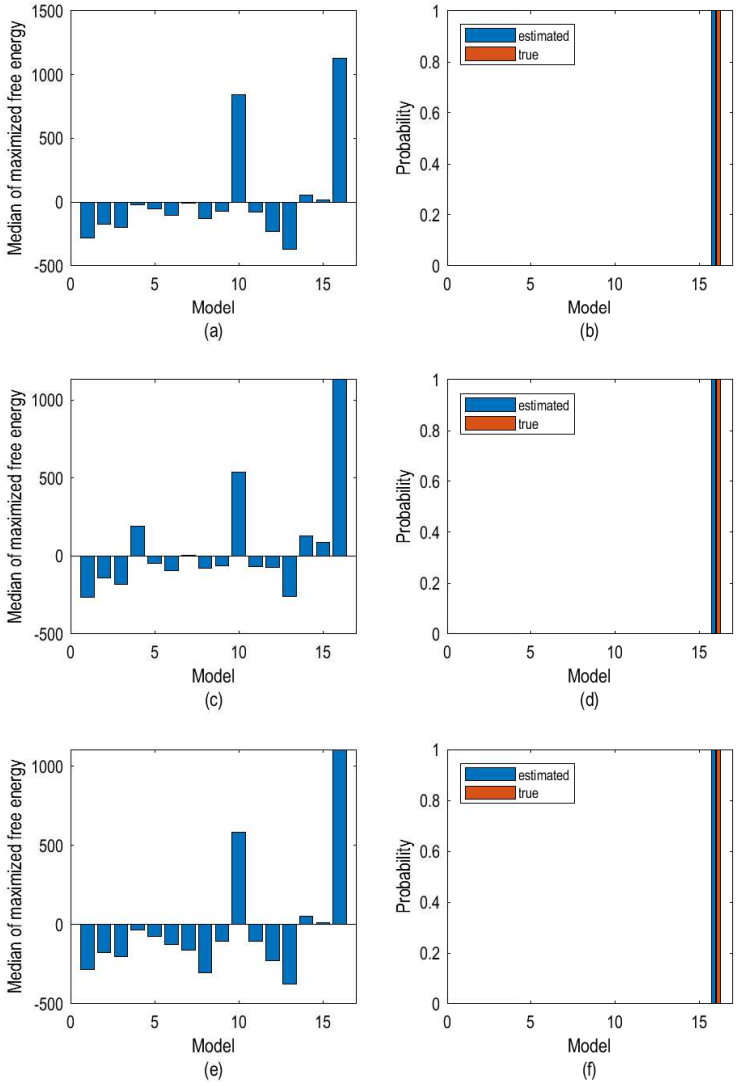

Figure 16. Bayesian model comparison in terms of the median of maximized free energy over 100 trials and the model posterior probability using **(a-b)** L-DCM, **(c-d)** D-DCM and **(e-f)** DCM for the ground truth M16$_s$ is the ground truth) in the context of bidirectional influence.

S3: Bayesian model comparison for real signals

Model selection in terms of the median of the maximized free energy over 12 trials in ictal phase is given in Fig 17 for cPBM. All methods provide almost 100% model evidence to identify M5 as depicted in Fig. 17 based on the median of maximized free energy.

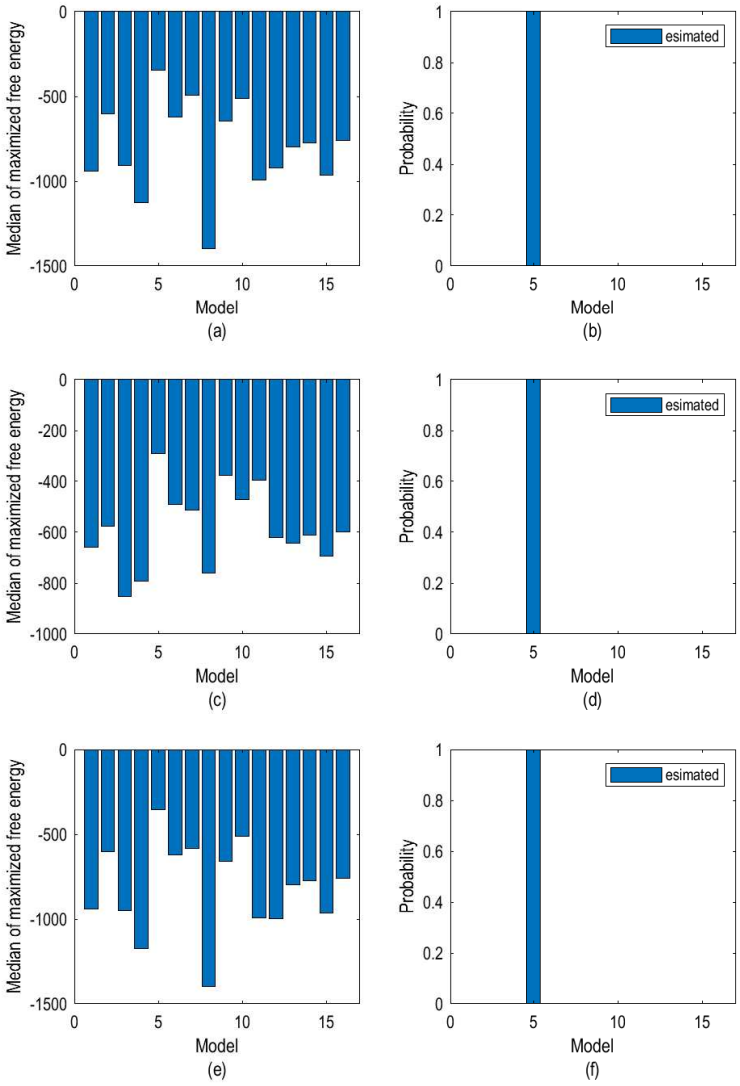

Figure 17. Bayesian model comparison in terms of the median of maximized free energy over 12 trials and the model posterior probability using **(a-b)** L-DCM, **(c-d)** D-DCM and **(e-f)** DCM for the Ictal phase in the context of real signals.